SCIENTIFIC REPORTS

OPEN

The influence of ionic strength on carbonate-based spectroscopic barometry for aqueous fluids: an *in-situ* Raman study on Na$_2$CO$_3$-NaCl solutions

Jia Wu[1], Shixia Wang[2] & Haifei Zheng[3]

The Raman wavenumber of the symmetric stretching vibration of carbonate ion (ν_1-CO$_3{}^{2-}$) was measured in three aqueous solutions containing 2.0 mol·L^{-1} Na$_2$CO$_3$ and 0.20, 0.42, or 0.92 mol·L^{-1} NaCl, respectively, from 122 to 1538 MPa at 22 °C using a moissanite anvil cell. The ν_1 Raman signal linearly shifted to higher wavenumbers with increasing pressure. Most importantly, the slope of ν_1-CO$_3{}^{2-}$ Raman frequency shift ($\partial\nu_1/\partial P)_I$ was independent of NaCl concentration. Moreover, elevated ionic strength was found to shift the apparent outline of the carbonate peak toward low wavenumbers, possibly by increasing the proportion of the contact ion pair NaCO$_3{}^-$. Further investigations revealed no cross-interaction between the pressure effect and the ionic strength effect on the Raman spectra, possibly because the distribution of different ion-pair species in the carbonate equilibrium was largely pressure-independent. These results suggested that the ionic strength should be incorporated as an additional constraint for measuring the internal pressure of various solution-based systems. Combining the ν_1-CO$_3{}^{2-}$ Raman frequency slope with the pressure herein with the values for the temperature or the ionic strength dependencies determined from previous studies, we developed an empirical equation that can be used to estimate the pressure of carbonate-bearing aqueous solutions.

Raman spectroscopy is widely employed for pressure determination in various natural[1] or artificial environments[2,3] and is often coupled with hydrothermal diamond anvil cell (HDAC) in studies on high $P-T$ geological systems. In HDAC experiments, the pressure inside the sample chamber is usually determined by measuring the wavenumber shift of an internal ruby-[4] or quartz-based[5] calibrant. However, pressure over the critical point or the presence of water could trigger phase transition or dissolution of the crystal pressure gauge, making mineral spectroscopy infeasible[6]. To address these problems, the use of a solute-based barometer has been proposed. Similar to those of solid minerals, Raman vibrational modes of anions in aqueous solutions are also affected by changes in temperature and/or pressure. The Raman wavenumber of pure liquid water at room temperature has been reported to decline with elevated pressure at a slope $(\partial\nu_{3244}/\partial P)_T$ of -30.4 cm^{-1}·GPa^{-1}[7]. The Raman shift of the symmetric stretching of SO$_4{}^{2-}$ in 1 mol·L^{-1} (abbreviated as M, hereinafter) Na$_2$SO$_4$ solution has been shown to be pressure- and temperature-dependent, which can be described by the $P-T$ equation of $P = 190.44 \cdot (\Delta\nu_{981})_P + 0.0027 \cdot T^2 + 2.9019 \cdot T - 111.68$[8]. Schmidt[9] reported similar behaviors of sulfate ion under high P-T conditions in HDAC. The same sulfate-based barometer was used to estimate the internal pressure of a pure sulfate solution in a HDAC experiment[10]. The findings of these studies collectively indicated that pressure measurement based on the Raman shifts of solutes could yield very similar results as conventional methods that rely on spectroscopic characterization of crystal pressure gauges.

[1]State Key Laboratory of Petroleum Resources and Prospecting — College of Geoscience, China University of Petroleum, Beijing, 102249, PR China. [2]College of Science, University of Shanghai for Science and Technology, Shanghai, 200093, PR China. [3]Key Laboratory of Orogenic Belts and Crustal Evolution, Department of Geology, Peking University, Beijing, 100871, PR China. Correspondence and requests for materials should be addressed to J.W. (email: jia.wu@cup.edu.cn)
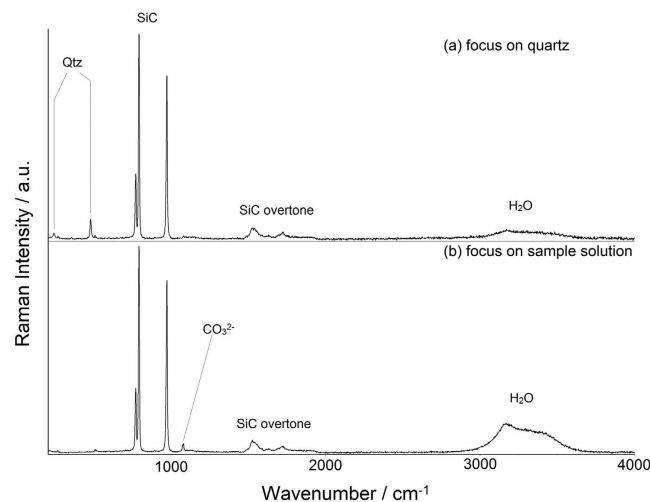
Figure 1. Representative Raman spectra of the pressure gauge (quartz) and the solution samples in the moissanite anvil cell. The scanned region spans the wavenumber range of 50–4000 cm^{-1}. (**a**) Laser beam is focused on the quartz. Raman signals at 206 and 464 cm^{-1} are attributed to quartz (Qtz); (**b**) Laser beam is focused on the Na$_2$CO$_3$-NaCl-H$_2$O solution. Raman signals assigned to the sample and moissanite anvil are respectively annotated. The Raman wavenumber of ν_1-CO$_3^{2-}$ in the solution is around 1066 cm^{-1}. The Raman band of water covers the region from 3000 to 3700 cm^{-1}. The moissanite signals include the shifts at 768 cm^{-1}, 789 cm^{-1}, and 967 cm^{-1}, as well as their overtone bands from 1400 to 1900 cm^{-1}.

Carbonate-bearing hydrothermal fluids are widely present in subduction zones or sedimentary basins[11,12]. Because of this, carbonate-based solutions are frequently used as a close approximant of H$_2$O and CO$_2$ mixed fluids in Raman spectroscopyic studies on geological phenomena under high *P-T* conditions. The shift of the ν_1-CO$_3^{2-}$ Raman line in aqueous solution toward higher wavenumbers with increasing pressure or decreasing temperature has been well documented by several research groups, including Wu and Zheng[13] and Schmidt[14]. Frantz[15] demonstrated that the speciations of both K$_2$CO$_3$ and KHCO$_3$ solutions varied with temperature by analyzing the characteristic Raman peaks of aqueous CO$_3^{2-}$ and HCO$_3^{-}$ up to 200 MPa and 550 °C. Although these results hinted at the potential value of using the characteristic Raman peak of CO$_3^{2-}$ as an alternative barometer for determining the pressure of a hydrostatic system, it should be pointed out that carbonate species, in their native geological environments, almost always coexist with a high level of Cl^{-} and various other electrolytes. Their interactions could influence the Raman lines of other Raman-active species[16]. Based on this principle, Sun, *et al.*[17] developed a calibration equation to estimate salt concentrations in aqueous solutions. A noticeable disadvantage of this approach is that solutes such as CO$_3^{2-}$ or SO$_4^{2-}$ can also modify the OH stretching bands of H$_2$O, resulting in an overestimation of Cl^{-}[18]. Moreover, Raman spectra of Na$_2$CO$_3$ in aqueous solutions could be modified by the concentration of different electrolytes[19,20]. Taken together, these results suggested that further studies on the relationship between Raman shift and solution composition would be necessary to enable Raman shifts of solutes as a reliable barometer.

Although there is mounting evidence indicating that the Raman shifts of CO$_3^{2-}$ are affected by a combination of environmental factors such as pressure, temperature, and salt concentration, no systematic studies have been conducted. Herein we report the *in-situ* Raman spectroscopic measurement of several Na$_2$CO$_3$-NaCl solution systems at high pressure levels (up to 1538 MPa) and ambient temperature (22 °C). The aim of this study is to examine the dependence of the Raman shift of CO$_3^{2-}$ on pressure in the presence of different concentrations of Cl^{-} and to develop a pressure equation.

Results

Because Raman scattering intensity of dispersed solute molecules is inherently weaker than that of crystals composed of the same compound, a high concentration of Na$_2$CO$_3$ was necessary to generate sufficiently strong Raman signals. We therefore set the concentration of Na$_2$CO$_3$ at 2 M, which was recommended by earlier studies[21]. Figure 1 shows the combined Raman spectra of the quartz pressure sensor and the sample solution in the wavenumber range of 50 to 4000 cm^{-1}. The moissanite anvil was responsible for the strongest peaks located at 768, 789, and 967 cm^{-1} as well as the overtone bands from 1400 to 1900 cm^{-1}[22], whereas quartz showed characteristic Raman lines at 206 and 464 cm^{-1}, with the latter being more intense. The single Raman peak at 1066 cm^{-1} was assigned to the symmetric stretching mode of carbonate ions[19], and the broad band from 3000 to 3700 cm^{-1} was attributable to the H–O vibration of water molecules[23,24].

For each solution, the internal pressure of the sample chamber was calculated from the Raman frequency shift of the 464-cm^{-1} line of quartz ($\Delta\nu_{464}$) using Eq. (3) (Table 1). The pressure was then plotted against the ν_1-CO$_3^{2-}$ Raman shift ($\Delta\nu_{1066}$) (Fig. 2). Regression analysis revealed a statistically significant linear relationship between pressure and $\Delta\nu_{1066}$ for each Na$_2$CO$_3$-NaCl solution (Table 2). The confidence interval was greater than 95% for all the analyses.

No. 1		No. 2		No. 3	
P/MPa	$\Delta\nu_{1066}$/cm^{-1}	P/MPa	$\Delta\nu_{1066}$/cm^{-1}	P/MPa	$\Delta\nu_{1066}$/cm^{-1}
122	0.8	122	0.4	134	0.5
145	1.0	145	0.5	190	0.7
156	1.2	201	0.9	257	0.5
246	1.7	190	1.0	540	2.5
336	1.8	336	1.4	632	2.8
678	3.5	483	2.3	678	3.2
771	4.3	759	3.6	887	4.0
957	5.2	724	3.7	968	4.9
1027	5.6	817	4.2	1109	5.8
1050	6.2	1027	5.7	1133	5.7
1168	6.0	1074	5.8	1216	6.7
1347	7.7	1204	5.8	1251	6.5
		1263	6.6	1394	6.3
		1323	6.7	1538	7.5
		1454	7.5		

Table 1. Raman shifts of ν_1-CO_3^{2-} with increasing pressure based on three Na_2CO_3-NaCl solutions.
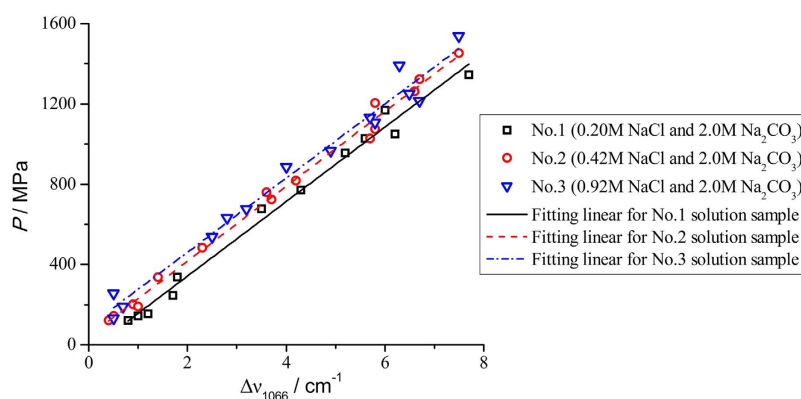
Figure 2. Pressures are plotted against the corresponding ν_1-CO_3^{2-} Raman shifts determined in this study. Three Na_2CO_3-NaCl solution samples are annotated as follows: No. 1: 0.20 M NaCl and 2.0 M Na_2CO_3, black squares, solid line; No. 2: 0.42 M NaCl and 2.0 M Na_2CO_3, red circles, dashed line; No. 3: 0.92 M NaCl and 2.0 M Na_2CO_3, blue triangles, dot-dashed line. All three samples are shown to have nearly identical pressure slopes for the ν_1-CO_3^{2-} Raman frequency. In addition, the Raman line shifts to lower frequencies as the concentration of NaCl increases.

Discussion

The results demonstrated a positive correlation between the Raman wavenumber of CO_3^{2-} and pressure at ambient temperature for the Na_2CO_3-NaCl-H_2O system (Fig. 2), which was consistent with previous findings obtained from similar high-pressure studies on solutions[14,21], liquid organic matters[25,26], and crystals[27,28]. The increase of the Raman frequencies at high pressure is primarily due to the lowered distance between molecules/ions and augmented force constants of various chemical bonds. Both this study and our previous investigation of the binary Na_2CO_3-H_2O system unveiled a positive correlation between pressure and the frequency of the ν_1-CO_3^{2-} Raman line with a slope $(\partial\nu_1/\partial P)_T$ of around 5.4 cm$^{-1}\cdot$GPa^{-1} at ambient temperature. It should be noted that several earlier studies on the correlations between pressure and the wavenumber of the ν_1 Raman line reported slightly different $(\partial\nu_1/\partial P)_T$ values (unit: cm$^{-1}\cdot$GPa^{-1}; 4.64[21], 5.06[15], 5.74[13]). Similar variation was also found for the pressure dependence of the ν_1-CH_4 Raman shift, which was summarized in details by Lu, *et al.*[29]. The discrepancy could be attributed to several possible factors, including pressure determination, Raman spectrograph calibration, and Raman shift of CH_4 under ambient *P-T* condition. On the other hand, the $(\partial\nu_1/\partial P)_T$ value of the ν_1-CO_3^{2-} Raman line is not only similar to that of the symmetric stretching vibration of sulfate in Na_2SO_4 solutions (1.54 M)[9], but also roughly on the same level as the pressure-dependent Raman frequency shift of commonly used crystal-based sensors such as ^{13}C diamond (2.8 cm$^{-1}\cdot$GPa^{-1}) and quartz (9 cm$^{-1}\cdot$GPa^{-1}). Based on Mantegazzi *et al.*'s[10] previous success in employing sulfate ion as a spectroscopic pressure sensor, we reasoned that aqueous carbonate ion could also serve as a barometer in similar systems.

Several groups have measured the wavenumber of the ν_1-CO_3^{2-} Raman line at varying concentrations. In order to simplify the expression for different cation species-bearing systems, we used ionic strength to describe

[Na₂CO₃]	[NaCl]	Fitting equation ($P = a\Delta\nu_{1066} + b$)			Standard error
mol·L⁻¹	mol·L⁻¹	Slope (MPa/cm⁻¹)	Intercept (MPa)	R²	MPa
2.01	0.20	185(6)	29(27)	0.988	14
2.00	0.42	187(4)	44(19)	0.993	11
1.99	0.92	185(8)	92(36)	0.978	18

Table 2. Quantification of the pressure influence on ν_1-CO₃²⁻ Raman shift in three Na₂CO₃-NaCl solutions. *P* is pressure in MPa. $\Delta\nu_{1066}$ is the relative ν_1-CO₃²⁻ Raman shift under pressure, and its value is between 0 and 10 cm⁻¹. The numbers in the brackets indicate the standard deviations (2σ) for the slope and the intercept. The standard errors (MPa) are calculated with the data in Table 1 and the fitting equations in Table 2.

Sources	[CO₃²⁻] mol·L⁻¹	[Cl⁻] mol·L⁻¹	$\partial\nu/\partial I$	R²	Standard error cm⁻¹
Oliver and Davis[19]	1.0−8.0ᵃ	0	−0.24	0.987	n.d.
Sun and Qin[30]	0.768−5.12ᵃ	0	−0.181	0.998	n.d.
	0.741 −1.56ᵇ	0	−0.063	0.993	0.033
	1.0ᵇ	0.5−2.0	−0.167	0.95	0.041
Sipos *et al.*[20]	0.1ᵇ	0.713−7.68*	−0.044I−0.058	0.996	n.d.
	0.1ᵇ	<4.7	~ −0.113	n.d.	n.d.

Table 3. Quantification of the ionic strength influence on ν_1-CO₃²⁻ Raman shift at ambient conditions based on previous references. ᵃPotassium carbonate solution. ᵇSodium carbonate solution. *Chloride anion is replaced by hydroxyl anion; n.d. indicates that the value is "not determined".

the influence of fluid composition on the ν_1-CO₃²⁻ Raman line. According to the Debye-Hückel theory of electrolytes, the total ionic strength (*I*) of a given aqueous solution can be calculated by the following equation:

$$I = \frac{1}{2}\sum z_i m_i^2$$

(1)

where z_i and m_i represent the concentration and charge of ion *I*, respectively. We opted for Eq. (1) as an approximate method for estimating the ionic strength of the Na₂CO₃-NaCl solutions in our study.

In Oliver and Davis[19]'s study of K₂CO₃ solutions from 1 to 8 M, the frequency was found to decline at a slope $(\partial\nu_1/\partial I)_{P,T}$ of −0.24 cm⁻¹·M⁻¹ (R² = 0.987) with regard to ionic strength. Consistent with these findings, Sun and Qin[30] reported that the $(\partial\nu_1/\partial I)_{P,T}$ slope for Na₂CO₃ solutions up to 15 wt% (1.556 M, I = 4.668 M) and K₂CO₃ solutions up to 50 wt% (5.125 M, I = 15.374 M) were −0.062 cm⁻¹·M⁻¹ (R² = 0.993) and −0.181 cm⁻¹·M⁻¹ (R² = 0.998), respectively (Table 3). On the other hand, the influence of ionic strength on Raman frequency might explain the slight variation that we previously observed among the three P-$\Delta\nu_{1066}$ equations derived from different Na₂CO₃ solutions[13]. There is substantial evidence to suggest that the fitting method we implemented should carry a theoretical uncertainty no greater than 0.15 cm⁻¹, which is considerably smaller than the actual difference among the three fitting equations[31,32].

There have also been efforts to determine the impact of coexisting ions, such as OH⁻ and Cl⁻, on the ν_1-CO₃²⁻ Raman spectrum[20]. These results were in satisfactory agreement with our experimental data. The ν_1-CO₃²⁻ Raman line at 0.100 M was indicated to shift to low frequency in the presence of NaOH, following a quadratic equation of $\nu_1 = -0.022I^2 - 0.058I + 1065.5$ (R² = 0.996). A similar trend was confirmed for 1.0 M Na₂CO₃ solutions when NaCl was added to a final concentration of 0.5 − 2.0 M; however, the decline of Raman wavenumber in this case exhibited a linear correlation with the Cl⁻ concentration at a slope $(\partial\nu_1/\partial I)_{P,T}$ of −0.113 cm⁻¹·M⁻¹[20], or −0.167 cm⁻¹·M⁻¹[30].

At low ionic strength, the interaction network of CO₃²⁻ in aqueous solution is dominated by its hydrogen bonding with solvent waters. Since the strength of the hydrogen bond only depends on the chemical nature of the bonding molecules, the Raman shift of CO₃²⁻ would remain relatively constant at low concentrations (e.g., 0.01 M and 0.1 M)[19]. As the concentration of CO₃²⁻ rises, however, electrostatic interactions between CO₃²⁻ and the surrounding cations would become more significant. The increase in the density of cations would encourage the formation of contact ion pairs (CIP), which, in the case of Na₂CO₃ solution systems, would be the binary species of NaCO₃⁻ due to the inability of Na⁺ to complex with CO₃²⁻[33]. The formation of CIP would weaken the π_4^6 bond of CO₃²⁻ and lower its force constant, causing the ν_1-CO₃²⁻ Raman line to shift to low wavenumbers. This hypothesis is supported by experimental results from several earlier studies. By using Na⁺ ion-selective glass electrode potentiometry, Capewell, *et al.*[34] demonstrated that the association constant of the reaction $Na^+(aq) + CO_3^{2-}(aq) \rightleftharpoons NaCO_3^-(aq)$ was inversely correlated with the total ionic strength of the solution. Schmidt[14], on the other hand, noticed the existence of large systematic residuals when attempting to perform a two-peak fitting on the 900–1200 cm⁻¹ region of the Raman spectrum of 1.6 M Na₂CO₃ solution obtained at 500 °C and 1.3 GPa. He subsequently eliminated the residuals by adopting a three-peak fitting strategy that entailed the assignment of the 1050 cm⁻¹ peak to the elusive NaCO₃⁻ species. However, this method is feasible only at elevated pressure and temperature, where the formation of HCO₃⁻ and NaCO₃⁻ is comparatively more
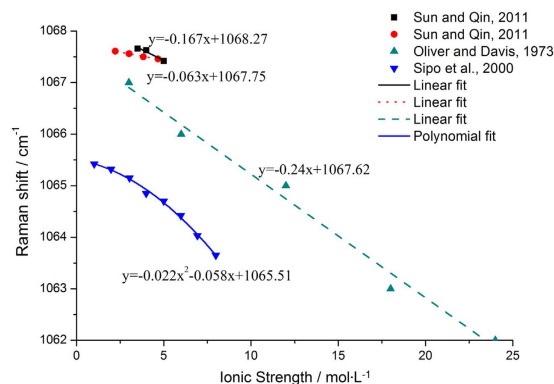
Figure 3. **The ν_1-CO_3^{2-} Raman line shifts to low wavenumbers with increasing ionic strength in pure or mixed carbonate sodium solutions (Square: 1 M Na_2CO_3 and 0.5–2.0 M NaCl; Round: 0.741–1.556 M Na_2CO_3; Triangle: 1–8 M Na_2CO_3; Inverted triangle: 0.1 M Na_2CO_3 and 0.713–7.681 M NaOH).** The relationships between Raman frequencies and ionic strengths are fitted as linear equations for the first three samples and as a quadratic equation for the last sample, respectively. The fitting results indicate that the correlation between ν_1-CO_3^{2-} Raman frequencies and ionic strengths is influenced by anion species in solution systems.

favorable from a thermodynamic standpoint[15]. In the current study, we argue that the relative proportion of the $NaCO_3^-$ peak is correlated to the wavenumber shift of the ν_1-CO_3^{2-} Raman line, the latter of which can therefore be used to evaluate the ionic strength effect.

A comparison among the results from different studies, as summarized in Fig. 3, indicated that although the introduction of additional anions always caused the ν_1-CO_3^{2-} Raman peak to shift toward low wavenumbers, the extent of the shift $(\partial \nu_1/\partial I)_{P,T}$ varied according to the specific type of anion. Among those examined, Cl^- was observed to have a more pronounced effect than the oxygen-containing anions. This was probably due to the fact that oxygen-containing anions tend to form solvent-separated (SSIP) or double solvent-separated ion pairs (2SIP) through hydrogen-bonding with solvent water molecules[35,36]; therefore, they are capable of attracting and sequestering a greater number of cations, making them less available for CIP formation with CO_3^{2-}. Unfortunately, the intrinsic complexity of solute-solute and solute-solvent interactions constitutes a formidable barrier for the reliable quantification of the ionic strength effect on Raman frequency shift. To simplify the problem, we took advantage of the fact Cl^- has the greatest abundance in various natural environments and generally plays a more significant role than the common oxygen-containing anions in Raman spectroscopy. Meanwhile, given that there have been well-established methods for quantifying salinity via freezing-point depression[37] or the Raman outline of water[38], it is feasible to estimate the Cl^- concentration in natural fluid systems. Thus, we decided to focus exclusively on the contribution of Cl^- to the Raman shift of CO_3^{2-} in subsequent analyses.

As illustrated in Fig. 2 and Table 2, the slope of Raman shift to pressure for the ν_1-CO_3^{2-} line was unaffected by the increase in the concentration of NaCl. This, combined with similar findings on pure Na_2CO_3 solutions in our previous study, suggested a lack of cross-interaction between pressure and ionic strength[13]. Therefore, the contribution of ionic strength to the Raman frequency shift of Na_2CO_3 in solution can be expressed as a simple linear equation. In order to determine the slope of Raman frequency with regard to ionic strength $(\partial \nu_1/\partial I)_{P,T}$, we opted to follow Sun and Qin[30]'s study on NaCl-Na_2CO_3 solution systems based on two considerations: i) The Raman spectra in their study were collected over a relatively long scanning period (30 sec), which we believed should lead to better measurement accuracy; ii) The NaCl-Na_2CO_3 solutions used in their study closely resembled the samples that we investigated in composition. Based on their experimental data, we concluded that for pure Na_2CO_3 solution, the correlation between its Raman shift and the ionic strength could be expressed as $(\partial \nu_1/\partial I)_{P,T} = -0.0625 \cdot \Delta I$, where $\Delta I = I - I^\theta = I - 3.0$ (unit: M, hereinafter for ionic strength) and $2.22 \leq I \leq 4.67$ (I^θ indicates the ionic strength of the standard Na_2CO_3 solution at 1 M). Additionally, NaCl-dependent Raman frequency shift was calculated to be $-0.167 \cdot I_{NaCl}$, where $0.5 \leq I_{NaCl} \leq 2.0$. One drawback in Sun and Qin's study was the narrow range of ionic strength that they investigated; as a result, the maximum contribution of ionic strength to ν_1-CO_3^{2-} Raman frequency shift was estimated to be around 0.2 cm^{-1}, which is roughly on the same level as the system error. Still, it has been suggested elsewhere that this linear relationship could be applied to solution systems with much greater ionic strength (up to $I = 24.0$)[19].

Several other groups have quantified the slope of ν_1-CO_3^{2-} Raman line shift with temperature. For example, its temperature dependence at 1 GPa and in the range of 100–275 °C was calculated to be approximately -0.041 cm$^{-1} \cdot$ °C^{-1} [21] (Table 4). However, due to the tendency of quartz dissolution in superheated aqueous solutions[39,40], it is impossible to eliminate the quartz contamination on the estimation of the thermal dependence of the ν_1-CO_3^{2-} Raman spectrum if quartz were used as the pressure indicator in HDAC. Frantz's experiment design involved the use of a hydraulic pump to control the pressure of the sample chamber, which offered several advantages over the conventional DAC system[41]. First, the pump provided enhanced pressure stability during each spectral analysis, with a maximum fluctuation of 10 bars, whereas DAC is generally incapable of maintaining an isobaric condition when the sample chamber is heated. Second, Frantz measured the pressure of the system

Sources	[CO_3^{2-}] mol·L^{-1}	P/MPa	Fitting equation ($\nu_{1066} = a \cdot T + b$)		R^2	Standard error cm^{-1}
			$\partial\nu/\partial T$	Intercept		
Frantz[15a]	1.0	100	−0.0452	1072.4	0.997	0.14
	1.0	150	−0.0446	1072.7	0.997	0.13
	1.0	200	−0.0440	1072.9	0.997	0.12
Martinez et al.[21b]	2.0	1000	−0.0411	1072.8	0.97	n.d.

Table 4. Quantification of the temperature influence on ν_1-CO_3^{2-} Raman shift based on previous references. ν_{1066} is in cm^{-1}. It is the carbonate Raman shift under a constant pressure P (MPa). T is temperature in °C, and its value ranges [a] from 24 to 550 °C, and [b] from 100 to 275 °C. The standard deviations for the slope and the intercept are not determined. [a]Potassium carbonate solution. [b]Sodium carbonate solution; n.d. indicates that the value is "not determined".

with a pressure meter, which could lead to better accuracy and more reliable performance. It should also be noted that Frantz conducted the Raman spectroscopic study over a wide temperature range (from room temperature to 550 °C). Therefore, we relied on Frantz[15]'s data, which reported a global value of −0.0446 cm^{-1}·°C^{-1} for the temperature dependence of the Raman shift (($\partial\nu_1/\partial P)_T$. Table 4).

The pressure- and temperature-dependence of Raman frequency have also been scrutinized in various other solid- and solution-based systems. Frantz[15] reported that the ν_1-CO_3^{2-} Raman line shifted toward low wavenumbers with increasing temperatures at a rate $(\partial\nu_1/\partial T)_P$ that was largely pressure-independent. The ν_1-SO_4^{2-} Raman line was shown to shift toward low wavenumbers with increasing pressure at a linear rate $(\partial\nu_1/\partial P)_T$ of 0.19 cm^{-1}·GPa^{-1}[8]. Similarly, the Raman frequency of quartz and sphalerite exhibited an inverse linear relationship with pressure at a slope $(\partial\nu_1/\partial P)_T$ that was mostly uniform within the temperature range tested[5,27]. Previous empirical fitting equations in Raman studies demonstrated that the cross-derivatives of the frequency shifts of Raman lines to the pressure and the temperature could be assumed as zero[42]. Therefore, we reasoned that the thermal effect can be expressed as a simple linear relationship between temperature and the Raman of ν_1-CO_3^{2-} wavenumber with no cross-interaction with the pressure effect.

No systematic analyses have been performed to investigate whether there is interplay between temperature and ionic strength in their influence on Raman spectra of Na_2CO_3 solutions. To circumvent this problem, we compared the isobaric temperature slopes $(\partial\nu_1/\partial T)_P$ for the Raman line of SO_4^{2-} separately obtained by Schmidt[9] and Qiao, et al.[8], both of whom measured the spectra in DAC with quartz as the pressure gauge. In Schmidt[9]'s study using a solution containing 1.54 M Na_2SO_4, the slope was calculated to be −0.0231 cm^{-1}·°C^{-1} at 322 MPa and in the range of 21–400 °C exhibited (R^2 = 0.9985), whereas Qiao, et al.[8] reported a result of −0.0224 cm^{-1}·°C^{-1} at 340 MPa and 100–250 °C for 1 M solution. However, according to Rull, et al.[43]'s estimation, the presence of an additional 0.54 M SO_4^{2-} would cause a Raman frequency shift of 0.2 cm^{-1}. It can be seen that the difference between the two slopes, which represents the interaction between the temperature effect and the ionic strength effect on Raman frequency, is almost negligible compared to the Raman shift of SO_4^{2-} generated from the increase of ionic strength alone. Similarly, this difference was also rather insignificant when compared to the change of Raman frequency caused by temperature variation. Therefore, we tentatively concluded that given the instrumental uncertainties in typical high-pressure Raman spectroscopic measurement, the cross-interaction between temperature and ionic strength could be safely omitted when estimating their impact on the Raman frequency of solutes.

Based on our experiment results and discussions detailed above, the empirical equation describing the correlation among pressure, temperature, ionic strength and the ν_1-CO_3^{2-} Raman characteristic frequency at 1066 cm^{-1} in aqueous solution can be expressed as follows:

$$
\begin{aligned}
P &= \left(\frac{\partial P}{\partial \nu_1}\right)_{T,I} \cdot \Delta\nu_{1066}(T, I) \\
&= \left(\frac{\partial P}{\partial \nu_1}\right)_{T,I} \cdot \left(\nu_1 - \nu_1^\theta - \left(\frac{\partial \nu_1}{\partial T}\right)_{P,I} \cdot \Delta T - \left(\frac{\partial \nu_1}{\partial I_{Na_2CO_3}}\right)_{P,T} \cdot \left(I_{Na_2CO_3} - I^\theta_{Na_2CO_3}\right) \right. \\
&\quad \left. - \left(\frac{\partial \nu_1}{\partial I_{NaCl}}\right)_{P,T,Na_2CO_3} \cdot I_{NaCl} \right) \\
&= 186 \cdot (\nu_1 - \nu_1^\theta + 0.0446 \cdot (T - 25) + 0.0625 \cdot (I_{Na_2CO_3} - 3.0) \\
&\quad + 0.167 \cdot I_{NaCl}) \\
P &= 186 \cdot (\nu_1 - \nu_1^\theta + 0.0446 \cdot T + 0.1875 \cdot [Na_2CO_3] \\
&\quad + 0.167 \cdot [NaCl] - 1.3025)
\end{aligned}
\tag{2}
$$

where P, T, and I represent the pressure (MPa), temperature (°C), and the ionic strength of the solution system (M), respectively; [X] indicates the concentration of the solute X (M); ν_1 and ν_1^θ denote the ν_1-CO_3^{2-} Raman

wavenumber measured under experimental conditions and standard conditions (as defined by 0.1 MPa, 25 °C, and 1.0 M Na_2CO_3 solution), respectively (cm^{-1}).

The standard error of Eq. (2) is derived from the fitting uncertainties of temperature, the concentration of Na_2CO_3, and the concentration of NaCl, whose contributions are ± 0.13, ± 0.03, and ± 0.04 (all in cm^{-1}), respectively. Since there is no cross-interaction between any two of these three variables, the overall standard error of Eq. (2) should be ± 0.20 cm^{-1}, which corresponds to a deviation of 37 MPa for the calculated pressure. On the other hand, the maximum standard error for the linear fitting equation shown in Table 2 is 18 MPa. Therefore, the theoretical maximum error generated from the calculation of pressure via Eq. (2) is less than 37 MPa. Obviously, the ionic strength effect can also be incorporated into ν_1^{θ} to afford $\nu_1^{\theta'}$, which denotes the Raman wavenumber of CO_3^{2-} in the fluid sample (as opposed to in 1.0 mol·L^{-1} Na_2CO_3 solution) under the standard P-T conditions. As a result, Eq. (2) can be rewritten as below:

$$P = 186 \cdot (\nu_1 - \nu_1^{\theta'} + 0.0446 \cdot (T - 25))$$

The equation that we have developed in this study has several practical ramifications for pressure determination in various natural and artificial fluid inclusions. To begin with, the equation contains additional terms for quantifying the impact of ionic strength on the Raman shift of Na_2CO_3. As an example, it can be inferred from the equation that the presence of 2 M NaCl in the solution can result in a deviation of 62 MPa in the calculated pressure, which exceeds the maximum theoretical error of 37 MPa mentioned above. This highlights the importance of incorporating ionic strength as an additional variable when calculating the internal pressure of various fluid systems. Natural fluid inclusions frequently contain daughter minerals that are formed by cooling and depressurization as a result of stratum exhumation during following geological evolution. When these fluids were analyzed in high P-T experiment settings, the daughter minerals could re-dissolve, increasing the ionic strength of the resultant solution and consequently causing pressure calculation errors. The impact of mineral contamination on pressure measurement could potentially be quantified and even corrected based on the strategy that we proposed in this study.

In addition, the equation also allows one to evaluate the impact of excess salinity on the accuracy of pressure measurement at different depths. A previous study conducted by Mao *et al.* estimated the overall relative uncertainty of ruby to be around $\pm 6\%$[44]. Therefore, the systematic offset resulting from the ionic strength of a 2 M NaCl solution (~ 10.5 wt%) would cause a similar level of relative uncertainty when the internal pressure of the fluid inclusion to be measured is around 1 GPa (an uncertainty of 6%), which corresponds to a depth of ~30 km below ground. Obviously, the contribution of this error would become substantially more significant when the fluid inclusion is found at a shallower depth, at which point any meaningful pressure measurement would be rendered impractical. This poses a particular challenge to the geological characterization of sedimentary basins located within a depth of 10 km to the ground level, which are often more enriched with fluids compared to magma chambers or subduction zones in the upper mantle or below. Raman measurements performed on these fluid systems often required stringent pressure calibration and higher spectral resolution. For example, the density and pressure of CH_4-H_2O system can be calculated from the Raman shift ν_1-CH_4 and P-V-T equations. Increased resolution of the Raman spectrum (± 0.3 cm^{-1}) was shown to result in a lower uncertainty of the pressure calculation (down to 3 MPa)[29], which is acceptable even at a depth of 3 km (~30 MPa of hydrostatic condition).

The physicochemical properties of aqueous fluids under high P-T conditions are indispensable for investigating geochemical behaviors at great depths[2]. Because of the inherent complexity of natural fluid inclusions, aqueous solutions of Na_2CO_3 or Na_2SO_4 have often been used as simplified model systems[9,10,14]. However, when performing laboratory studies on these solutions, the high P-T conditions can cause conventional crystal-based pressure gauges to partially dissolve, leading to altered fluid compositions. For example, the solubility of quartz increases dramatically from 0.78 wt% at 500 °C and 5 kbar to 12.56 wt% at 900 °C and 10 kbar[45]. This problem can be addressed by replacing the conventional pressure gauges with a solute-based barometer when the high P-T experiments are performed under conditions that could potentially trigger undesirable side reactions or cause the crystal calibrants to dissolve.

In short, the current study supports that alterations in fluid salinity could have a significant impact on ionic interaction[9], mineral solubility[46], as well as the P-V-T diagrams of various aqueous systems[47]. Since NaCl is the most significant contributor to the ionic strength in natural fluid inclusions, we argue that it should be considered as a necessary, or even essential, component in laboratory investigations of artificial electrolytic solutions, such as Na_2CO_3- and Na_2SO_4-based systems, in order to more accurately characterize the physicochemical behaviors of aqueous fluids at natural geological settings. Meanwhile, we are convinced that our carbonated-based barometer adds to the current arsenal of pressure sensors for *in-situ* spectroscopic observation under high P-T conditions.

Methods

In order to probe the effect of Cl$^-$ on the Raman spectrum of CO_3^{2-}, three solutions consisting of 2 M Na_2CO_3 with three concentrations of NaCl (0.20, 0.42, and 0.92 M) were prepared in distilled water and each set to a final volume of 50 mL in a volumetric flask. High-pressure experiments were conducted in a moissanite anvil cell modified from a diamond anvil cell (DAC)[48]. The sample chamber comprised a 0.3 mm diameter hole drilled in the center of a 0.5 mm thick stainless steel gasket and flanked between the two anvils. A small piece of quartz was placed as an internal pressure gauge in the sample chamber, where the aqueous sample solution was also enclosed. The Raman spectra of the quartz and the sample were separately measured in the wavenumber range of 50–4000 cm^{-1} using a Raman microspectrometer (with a spectral resolution of ± 1 cm^{-1}, Renishaw system RM-1000, Renishaw Group, Gloucestershire, United Kingdom) equipped with a charged coupled detector and a Leitz 20X working objective. A 25 mW argon laser (514.5 nm) was used for sample excitation. The slit width and the collection time were set to 50 μm and 10 s, respectively. All measurements were performed at ambient

temperature (approximately 22 °C) and under the pressure range of 100–1600 MPa. A three-minute interval was introduced immediately after each pressure change between two consecutive measurements in order for the sample to regain equilibrium. Peakfit4 was used to fit the Raman spectrum of quartz in the range of 300–600 cm^{-1} and of CO_3^{2-} in the range of 1000–1200 cm^{-1} into Gaussian peaks, from which spectrometric parameters such as wavenumber were derived.

The internal pressure in the experimental volume inside the diamond anvil cell was determined using the shift of the most intense Raman band of quartz near 464 cm^{-1} using the calibration equation[5]:

$$P = 0.36079 \times \left[(\Delta\nu_P)_{464} \right]^2 + 110.86 \times (\Delta\nu_P)_{464} \tag{3}$$

where $(\Delta\nu_P)_{464}$ indicates the pressure-induced frequency shift for the characteristic Raman peak of quartz from the standard value of 464 cm^{-1} measured under ambient conditions. It should be noted that equation (3) would yield a measurement uncertainty of ± 50 MPa and its application should be limited to $0 < (\Delta\nu_P)_{464} \leq 20$ cm^{-1} and $P < 2.0$ GPa.

References

1. Zheng, H., Duan, T., Sun, Q. & Qiao, E. A potential geological barometer: new method to determine the pressure with daughter minerals in fluid inclusion by Raman spectroscopy. *Advance in Earth Sciences* 804–808 (2005).
2. Roedder, E. & Bodnar, R. J. Geologic pressure determinations from fluid inclusion studies. *Annu Rev Earth Pl Sc* **8**, 263–301 (1980).
3. Burke, E. A. J. Raman microspectrometry of fluid inclusions. *Lithos* **55**, 139–158 (2001).
4. Mao, H. K., Xu, J. & Bell, P. M. Calibration of the ruby pressure gauge to 800-kbar under quasi-hydrostatic conditions. *Journal of Geophysical Research-Solid Earth and Planets* **91**, 4673–4676 (1986).
5. Schmidt, C. & Ziemann, M. A. *In-situ* Raman spectroscopy of quartz: A pressure sensor for hydrothermal diamond-anvil cell experiments at elevated temperatures. *Am Mineral* **85**, 1725–1734 (2000).
6. Zheng, H., Sun, Q., Zhao, J. & Duan, T. Comment on the pressure gauge for the experiments at high temperature and high pressure with DAC. *Chinese Journal of High Pressure Physics* **18**, 5 (2004).
7. Li, M. & Zheng, H. Research on Raman spectra of water as a pressure gauge at high pressure and room temperature. *Chinese Journal of High Pressure Physics* **18**, 5 (2004).
8. Qiao, E., Duan, T. & Zheng, H. Study of pressure gauge for fluid inclusions: Raman spectroscopy of Na_2SO_4 solution at high temperature and high pressure. *Acta Mineralogica Sinica* **26**, 4 (2006).
9. Schmidt, C. Raman spectroscopic study of a $H_2O + Na_2SO_4$ solution at 21–600 °C and 0.1 MPa to 1.1 GPa: Relative differential ν_1-SO_4^{2-} Raman scattering cross sections and evidence of the liquid-liquid transition. *Geochimica Et Cosmochimica Acta* **73**, 425–437 (2009).
10. Mantegazzi, D., Sanchez-Valle, C., Reusser, E. & Driesner, T. Thermodynamic properties of aqueous sodium sulfate solutions to 773 K and 3 GPa derived from acoustic velocity measurements in the diamond anvil cell. *J Chem Phys* **137** (2012).
11. Thomas, R., Davidson, P. & Schmidt, C. Extreme alkali bicarbonate- and carbonate-rich fluid inclusions in granite pegmatite from the Precambrian Ronne granite, Bornholm Island, Denmark. *Contributions to Mineralogy and Petrology* **161**, 315–329 (2011).
12. Navon, O. High internal-pressures in diamond fluid inclusions determined by infrared-absorption. *Nature* **353**, 746–748 (1991).
13. Wu, J. & Zheng, H. Raman spectra of carbonate ions as pressure gauge at high pressure and room temperature. *Spectrosc Spect Anal* **29**, 690–693 (2009).
14. Schmidt, C. Raman spectroscopic determination of carbon speciation and quartz solubility in $H_2O + Na_2CO_3$ and $H_2O + NaHCO_3$ fluids to 600 °C and 1.53 GPa. *Geochimica Et Cosmochimica Acta* **145**, 281–296 (2014).
15. Frantz, J. D. Raman spectra of potassium carbonate and bicarbonate aqueous fluids at elevated temperatures and pressures: comparison with theoretical simulations. *Chemical Geology* **152**, 211–225 (1998).
16. Dubessy, J., Lhomme, T., Boiron, M. C. & Rull, F. Determination of chlorinity in aqueous fluids using Raman spectroscopy of the stretching band of water at room temperature: Application to fluid inclusions. *Appl Spectrosc* **56**, 99–106 (2002).
17. Sun, Q., Zhao, L., Li, N. & Liu, J. Raman spectroscopic study for the determination of Cl^- concentration (molarity scale) in aqueous solutions: Application to fluid inclusions. *Chemical Geology* **272**, 55–61 (2010).
18. Wang, X., Hu, W. & Chou, I.-M. Raman spectroscopic characterization on the OH stretching bands in $NaCl-Na_2CO_3-Na_2SO_4-CO_2$-$H_2O$ systems: Implications for the measurement of chloride concentrations in fluid inclusions. *J. Geochem. Explor.* **132**, 111–119 (2013).
19. Oliver, B. G. & Davis, A. R. Vibrational spectroscopic studies of aqueous alkali metal bicarbonate and carbonate solutions. *Canadian Journal of Chemistry* **51**, 698–702 (1973).
20. Sipos, P., Bolden, L., Hefter, G. & May, P. M. Raman spectroscopic study of ion pairing of alkali metal ions with carbonate and sulfate in aqueous solutions. *Aust J Chem* **53**, 887–890 (2000).
21. Martinez, I., Sanchez-Valle, C. & Daniel, I. & Reynard, B. High-pressure and high-temperature Raman spectroscopy of carbonate ions in aqueous solution. *Chemical Geology* **207**, 47–58 (2004).
22. Feldman, D. W., Parker, J. H., Choyke, W. J. & Patrick, L. Raman Scattering in 6H SiC. *Phys Rev* **170**, 698–704 (1968).
23. Walrafen, G. E. Raman spectral studies of water structure. *J Chem Phys* **40**, 3249–3256 (1964).
24. Walrafen, G. E. Raman spectral studies of effects of temperature on water structure. *J Chem Phys* **47**, 114–126 (1967).
25. Jian, X. & Zheng, H. Raman scattering spectroscopic study of n-tetradecane under high pressure and ambient temperature. *Spectroc. Acta Pt. A-Molec. Biomolec. Spectr.* **72**, 214–217 (2009).
26. Wang, H., Zheng, H. & Sun, Q. Raman spectroscopic studies of the phase transitions in hexane at high pressure. *Appl Spectrosc* **59**, 1498–1500 (2005).
27. Yang, Y., Zheng, H. & Zhang, L. Determining pressure with daughter minerals in fluid inclusion by Raman spectroscopy: sphalerite as an example. *Acta Geol Sin-Engl* **83**, 628–632 (2009).
28. Xu, J. A., Mao, H. K. & Bell, P. M. High-Pressure Ruby and Diamond Fluorescence - Observations at 0.21 to 0.55 Terapascal. *Science* **232**, 1404–1406 (1986).
29. Lu, W. J., Chou, I. M., Burruss, R. C. & Song, Y. C. A unified equation for calculating methane vapor pressures in the CH_4-H_2O system with measured Raman shifts. *Geochimica Et Cosmochimica Acta* **71**, 3969–3978 (2007).
30. Sun, Q. & Qin, C. Raman OH stretching band of water as an internal standard to determine carbonate concentrations. *Chemical Geology* **283**, 274–278 (2011).
31. Izraeli, E. S., Harris, J. W. & Navon, O. Raman barometry of diamond formation. *Earth Planet Sc Lett* **173**, 351–360 (1999).
32. Yamamoto, J. *et al.* Fossil pressures of fluid inclusions in mantle xenoliths exhibiting rheology of mantle minerals: implications for the geobarometry of mantle minerals using micro-Raman spectroscopy. *Earth Planet Sc Lett* **198**, 511–519 (2002).
33. Palmer, D. A. & van Eldik, R. The chemistry of metal carbonato and carbon dioxide complexes. *Chem Rev* **83**, 651–731 (1983).
34. Capewell, S. G., Hefter, G. & May, P. M. Potentiometric investigation of the weak association of sodium and carbonate ions at 25 °C. *J Solution Chem* **27**, 865–877 (1998).

35. Atkinson, G. & Petrucci, S. Ion association of magnesium sulfate in water at 25°. *The Journal of Physical Chemistry* **70,** 3122–3128 (1966).
36. Zhang, Y. & Chan, C. K. Study of contact ion pairs of supersaturated magnesium sulfate solutions using raman scattering of levitated single droplets. *J Phys Chem A* **104,** 9191–9196 (2000).
37. Bodnar, R. J. Revised equation and table for determining the freezing-point depression of H_2O-NaCl solutions. *Geochimica Et Cosmochimica Acta* **57,** 683–684 (1993).
38. Mernagh, T. P. & Wilde, A. R. The use of the laser raman microprobe for the determination of salinity in fluid inclusions. *Geochimica Et Cosmochimica Acta* **53,** 765–771 (1989).
39. Tian, F. Experimental studies on the application method of diamond anvil cell in metallogenesis investigation, Doctor thesis, Peking University (2012).
40. Friedman, II. The solubility of quartz in sodium carbonate solutions at high temperature. *J Am Chem Soc* **70,** 2649–2650 (1948).
41. Frantz, J. D., Dubessy, J. & Mysen, B. An optical-cell for Raman-spectroscopic studies of supercritical fluids and its application to the study of water to 500 °C and 2000 bar. *Chemical Geology* **106,** 9–26 (1993).
42. Gillet, P., Daniel, I., Guyot, F., Matas, J. & Chervin, J. C. A thermodynamic model for $MgSiO_3$-perovskite derived from pressure, temperature and volume dependence of the Raman mode frequencies. *Physics of the Earth and Planetary Interiors* **117,** 361–384 (2000).
43. Rull, F., Sobron, F. & Nielsen, O. F. Dependence on concentration and temperature of the dynamics of SO_4^{2-} in Li_2SO_4, Na_2SO_4 and K_2SO_4 aqueous-solutions studied by Raman-spectroscopy. *J Raman Spectrosc* **26,** 663–668 (1995).
44. Mao, H. K., Bell, P. M., Shaner, J. W. & Steinberg, D. J. Specific volume measurements of Cu, Mo, Pd, and Ag and calibration of the ruby R_1 fluorescence pressure gauge from 0.06 to 1 Mbar. *J Appl Phys* **49,** 3276–3283 (1978).
45. Manning, C. E. The solubility of quartz in H_2O in the lower crust and upper-mantle. *Geochimica Et Cosmochimica Acta* **58,** 4831–4839 (1994).
46. Newton, R. C. & Manning, C. E. Quartz solubility in H_2O-NaCl and H_2O-CO_2 solutions at deep crust-upper mantle pressures and temperatures: 2–15 kbar and 500–900 °C. *Geochimica Et Cosmochimica Acta* **64,** 2993–3005 (2000).
47. Mantegazzi, D., Sanchez-Valle, C. & Driesner, T. Thermodynamic properties of aqueous NaCl solutions to 1073 K and 4.5 GPa, and implications for dehydration reactions in subducting slabs. *Geochimica Et Cosmochimica Acta* **121,** 263–290 (2013).
48. Mao, H. K. & Bell, P. M. Design and varieties of the Megabar cell. *Carnegie Institute Washington Yearbook* **77,** 904 –908 (1978).

Acknowledgements

Author Contributions

J.W. and H.Z. designed research. J.W. and S.W. conducted experiments and analyzed the data. J.W. wrote the main manuscript. All authors reviewed the manuscript.

Additional Information

Competing financial interests: The authors declare no competing financial interests.

How to cite this article: Wu, J. *et al.* The influence of ionic strength on carbonate-based spectroscopic barometry for aqueous fluids: an *in-situ* Raman study on Na_2CO_3-NaCl solutions. *Sci. Rep.* **6**, 39088; doi: 10.1038/srep39088 (2016).

Publisher's note: Springer Nature remains neutral with regard to jurisdictional claims in published maps and institutional affiliations.